Available online at www.sciencedirect.com
ScienceDirect
Journal of Magnetic Resonance 184 (2007) 344–349
JMR Journal of Magnetic Resonance
www.elsevier.com/locate/jmr

Communication

Relayed ^{13}C magnetization transfer: Detection of malate dehydrogenase reaction in vivo

Jehoon Yang, Jun Shen *

Molecular Imaging Branch, National Institute of Mental Health Intramural Research Program, National Institutes of Health, 9000 Rockville Pike, Bethesda, MD 20892-1527, USA

Received 1 September 2006; revised 3 November 2006
Available online 27 November 2006

Abstract

Malate dehydrogenase catalyzes rapid interconversion between dilute metabolites oxaloacetate and malate. Both oxaloacetate and malate are below the detection threshold of in vivo MRS. Oxaloacetate is also in rapid exchange with aspartate catalyzed by aspartate aminotransferase, the latter metabolite is observable in vivo using ^{13}C MRS. We hypothesized that the rapid turnover of oxaloacetate can effectively relay perturbation of magnetization between malate and aspartate. Here, we report indirect observation of the malate dehydrogenase reaction by saturating malate C2 resonance at 71.2 ppm and detecting a reduced aspartate C2 signal at 53.2 ppm due to relayed magnetization transfer via oxaloacetate C2 at 201.3 ppm. Using this strategy the rate of the cerebral malate dehydrogenase reaction was determined to be 9 ± 2 μmol/g wet weight/min (means ± SD, $n = 5$) at 11.7 Tesla in anesthetized adult rats infused with [1,6-$^{13}C_2$]glucose.
Published by Elsevier Inc.

Keywords: In vivo MRS; Magnetization transfer; Malate dehydrogenase; Carbon-13; Enzymology

1. Introduction

Malate dehydrogenase (MDH; L-malate:NAD oxidoreductase; EC 1.1.1.37) catalyzes the reversible interconversion between L-malate and oxaloacetate using nicotinamide adenine dinucleotide (NAD) as a coenzyme

$$\text{L} - \text{malate} + \text{NAD}^+ \leftrightarrow \text{oxaloacetate} + \text{NADH} + \text{H}^+$$

The equilibrium of the MDH reaction energetically favors the reduction of oxaloacetate into malate. MDH is found in all eukaryotic cells as two isozymes: mitochondrial and cytoplasmic. The mitochondrial MDH is the final enzyme of the tricarboxylic acid (TCA) cycle. It oxidizes malate into oxaloacetate. Both mitochondrial and cytoplasmic MDH participate in the malate–aspartate shuttle which carries the reducing equivalents from the cytoplasm into the mitochondria for oxidation. In cytoplasm, MDH plays an important role in generating NADPH needed for reductive biosynthesis. The carbon skeleton of malate transported out of mitochondria is also utilized for gluconeogenesis.

Previously, applications of enzyme-specific in vivo magnetization (saturation or inversion) transfer spectroscopy were limited to ^{31}P MRS studies of creatine kinase and ATP exchange reactions [1,2]. Very recently, we discovered the in vivo magnetization transfer effect of aspartate aminotransferase (AAT) reaction. It was shown that the rapid and reversible AAT half-reactions (glutamate ↔ α-ketoglutarate and aspartate ↔ oxaloacetate) are detectable in vivo using ^{13}C magnetization transfer (CMT) by saturating the carbonyl carbon (C2) of either α-ketoglutarate at 206.0 ppm or oxaloacetate at 201.3 ppm [3]. The CMT effect of the lactate dehydrogenase (LDH) reaction (pyruvate + NADH + H^+ ↔ lactate + NAD^+) was similarly detected in vivo in bicuculline-treated rats and in glioma by saturating the pyruvate C2 resonance at 207.9 ppm [4]. Like AAT and LDH, MDH also catalyzes a near equilibrium reaction in vivo [5]. In the homogenate of adult

* Corresponding author. Fax: +1 301 480 2397.
E-mail address: shenj@intra.nimh.nih.gov (J. Shen).

1090-7807/$ - see front matter Published by Elsevier Inc.
doi:10.1016/j.jmr.2006.11.002

rat cerebral cortex, the activity of MDH (V_{max}) was determined to be 69 μmol/g wet weight/min [6]. Because of the extremely low in vivo concentration of oxaloacetate (approximately 0.005 μmol/g wet weight in rat brain, [5]) and the rapid AAT- and MDH-catalyzed reactions, there exists an interesting possibility of relaying perturbation of magnetization between malate and aspartate via the rapidly turning over oxaloacetate, which is shared by both reactions.

Altered MDH activity in the abnormal brain has been reported using postmortem analytical methods (e.g., [7]). The antipsychotic drug haloperidol has also been found to elevate the transcript-encoding of cerebral cytoplasmic MDH [8]. Due to the low in vivo concentration of malate (approximately 0.3–0.4 μmol/g wet weight in brain [5,9]), malate and the MDH reaction are generally considered to be beyond the capability of in vivo MRS. With the rapidly increasing number of high field magnets available for human and animal studies, it is desirable to further extend the scope of the "signal-hungry" in vivo MRS to include previously undetectable signals. Relayed ^{13}C magnetization transfer could offer a mean to probe the malate dehydrogenase reaction in vivo, by saturating the undetectable malate C2 at 71.2 ppm and detecting changes in the MRS-detectable aspartate C2 signal at 53.2 ppm. The successful in vivo demonstration of this strategy in isoflurane-anesthetized adult rat brain using an 11.7 Tesla scanner is presented here. The standard steady state saturation transfer method, which produces the maximum SNR, was employed to measure the rate of the MDH reaction. To the best of our knowledge, no in vivo measurement of the malate dehydrogenase-catalyzed exchange rate had been reported prior to the current work.

2. Theory

The following pseudo first order rate constants are defined: k_{MO} for malate → oxaloacetate; k_{OM} for oxaloacetate → malate; k_{OA} for oxaloacetate → aspartate; and k_{AO} for aspartate → oxaloacetate. The modified Bloch–McConnell equations for the longitudinal magnetization of malate, oxaloacetate and aspartate C2 carbons ([M], [O] and [A], respectively) are

$$d[M]/dt = ([M]_0[M])/T_{1M} + k_{OM}[O] - k_{MO}[M] \quad (1)$$

$$d[O]/dt = ([O]_0[O])/T_{1O} + k_{MO}[M] + k_{AO}[A] - (k_{OM} + k_{OA})[O] \quad (2)$$

$$d[A]/dt = ([A]_0[A])/T_{1A} + k_{OA}[O] - k_{AO}[A] \quad (3)$$

where T_{1M}, T_{1O} and T_{1A} are the spin–lattice relaxation times of malate, oxaloacetate and aspartate C2 carbons, respectively, in the absence of any chemical exchange, and $[M]_0$, $[O]_0$ and $[A]_0$ are the thermal equilibrium values of [M], [O] and [A], respectively. We further define that $V_{AAT} \equiv k_{AO}[A]_0 = k_{OA}[O]_0$ and $V_{MDH} \equiv k_{MO}[M]_0 = k_{OM}[O]_0$.

Eqs. (2) and (3) can be solved for the steady state condition $d[O]/dt = d[A]/dt = 0$ and $[M] = 0$ resulting from RF saturation of the malate C2 resonance at 71.2 ppm

$$[O]_{ss} = ([O]_0/T_{1O} + k_{AO}[A])/(T_{1O}^{-1} + k_{OM} + k_{OA}) \quad (4)$$

$$[A]_{ss}/[A]_0 = (T_{1A}^{-1} + \alpha)/(T_{1A}^{-1} + k_{AO} + \beta) \quad (5)$$

where $[O]_{ss}$ and $[A]_{ss}$ are the steady state magnetization of oxaloacetate and aspartate C2 resonances and

$$\alpha = k_{AO}/(1 + T_{1O}(k_{OM} + k_{OA})) \quad (6)$$

$$\beta = k_{OA}k_{AO}/(T_{1O}^{-1} + k_{OM} + k_{OA}) \quad (7)$$

The relationship $k_{AO}[A]_0 = k_{OA}[O]_0$ was used in deriving Eq. (5). Note that if $\alpha = \beta = 0$ Eq. (5) reduces to the well-known saturation transfer equation for two-site exchange ($[A]_{ss}/[A]_0 = T_{1A}^{-1}/(T_{1A}^{-1} + k_{AO})$, same as Eq. (11) in Ref. [2]).

Since $[O]_0 \ll ([M]_0, [A]_0)$, the turnover rate of oxaloacetate is expected to be several orders of magnitude greater than the longitudinal relaxation rate of its unprotonated carbonyl carbon. That is, $k_{OA} \gg T_{1O}^{-1}$. Therefore, Eq. (5) can be rewritten into

$$[\Delta A]/[A]_0 = k_{AO}/(k_{AO} + T_{1A}^{-1}(1 + V_{AAT}/V_{MDH})) \quad (8)$$

where $[\Delta A] \equiv [A]_0 - [A]_{ss}$. The relationship $k_{OA}/k_{OM} = V_{AAT}/V_{MDH}$ was also used in deriving Eq. (8). Since $k_{AO}[A] \gg [O]_0/T_{1O}$ and $k_{OM} + k_{OA} \gg T_{1O}^{-1}$, it can be shown from Eq. (4) that

$$[O]_{ss}/[O]_0 = ([A]_{ss}/[A]_0)/(1 + V_{MDH}/V_{AAT}). \quad (9)$$

3. Experimental methods

The experimental methods were similar to those used in our previous publications [3,4]. Briefly, all experiments were performed using a Bruker 11.7 Tesla spectrometer interfaced to an 89-mm bore vertical magnet and ParaVision 3.0.1 (Bruker Biospin, Billerica, MA). An in-house transmit/receive concentric surface ^{13}C (circular, diameter: 10 mm)/^{1}H (octagonal, diagonal: 25 mm) RF coil system was used which is integrated to an animal handling system [10]. Male Sprague–Dawley rats (167–186 g, $n = 8$) fasted for 24 h with free access to drinking water were studied to measure the relayed CMT effect ($n = 5$) and the T_1 relaxation rate of aspartate C2 resonance ($n = 3$) in the rat brain as approved by the National Institute of Mental Health (NIMH) Animal Care and Use Committee. The rats were orally intubated and ventilated with a mixture of 70% N_2O/30% O_2 and 1.5% isoflurane. The left femoral artery was cannulated for measuring arterial blood gases (pO_2, pCO_2), pH, plasma glucose concentration using a blood analyzer (Bayer Rapidlab 860, East Walpole, MA), and for monitoring arterial blood pressure. One femoral vein was also cannulated for intravenous infusion of [1,6-$^{13}C_2$]glucose (1-^{13}C, fractional enrichment: 0.99; 6-^{13}C, fractional enrichment: 0.97, Cambridge Isotope Laboratories, Andover, MA). The scalp was removed to minimize extracranial contamination of in vivo ^{13}C data. Intravenous infusion of [1,6-$^{13}C_2$]glucose was started approximately 1 h prior to in vivo ^{13}C data acquisition.

The infusion protocol consists of an initial bolus of 162 mg/kg/min of 1.1 M [1,6-$^{13}C_2$]glucose in the first five minutes followed by an approximately constant-rate infusion of the same glucose solution at ~63 mg/kg/min. The arterial blood was sampled every 60 min. The infusion rate was adjusted to maintain the plasma glucose level at 20–25 mM. Other system physiological parameters were maintained at normal range throughout the ^{13}C data acquisition period with few exceptions. End-tidal CO_2, tidal pressure of ventilation, and heart rate were also monitored. The body temperature was maintained at ~37.5 °C using an external pump for water circulation (BayVoltex, Modesto, CA).

Three-slice (coronal, horizontal and sagittal) scout RARE images (FOV = 2.5 cm, slice thickness = 1 mm, TR/TE = 200/15 ms, rare factor = 8, 128 × 128 data matrix) were acquired for positioning the integrated RF probe/animal handling system inside the Bruker Mini 0.5 gradient insert such that the gradient isocenter was about 0–1 mm posterior to bregma. The rat brain was shimmed as described previously using the FASTMAP/FLATNESS methods ([11] and references therein). The 90° excitation, surface-coil-localized, interleaved acquisition method was used to measure the relayed CMT effect [3,4]. A 1-ms adiabatic half-passage pulse was used for non-selective 90° ^{13}C excitation [12] TR = 7.6 s. The WALTZ-4 scheme based on a 400 μs nominal 90° rectangular pulse was used for proton decoupling. The decoupling pulse train was executed for 106 ms. Broadband $^{1}H \rightarrow {}^{13}C$ nuclear Overhauser enhancement was generated using a train of non-selective hard pulses with a nominal flip angle of 180° spaced 100 ms apart. When the relayed ^{13}C magnetization transfer spectra were acquired, the malate C2 at 71.2 ppm was saturated using a train of spectrally selective 2-ms Gaussian pulses with a nominal flip angle of 180° spaced 12 ms apart. The duration of the Gaussian pulse train was 7244 ms. When the control spectra were acquired, the saturating pulse train was placed at an equal spectral distance from aspartate C2 at 53.2 ppm but on the opposite side of malate C2. The saturated and control spectra were interleaved every FID. Data were zerofilled to 16 K. The ^{13}C signals in the 53–56 ppm region were analyzed using the MATLAB curve-fitting toolbox (The MathWorks, Inc., Natick, MA) in the frequency domain. The inversion-recovery null of aspartate C2 without saturating either oxaloacetate C2 or malate C2 was measured using the inversion-recovery null method. A 4-ms hyperbolic secant inversion pulse (phase factor = 5, 1% truncation) and a nominal 60° excitation pulse were used. Full inversion was verified by matching the intensity of ^{13}C signals without the inversion pulse with that acquired with the inversion pulse but without any inversion-recovery delay TR = 6.4 s. The parameters for generation of $^{1}H \rightarrow {}^{13}C$ nuclear Overhauser enhancement and ^{1}H decoupling used in the T_1 null measurement were the same as described above. The ^{13}C carrier frequency was centered near aspartate C2.

4. Results

The magnetization transfer pulse sequence described in Section 3 was first tested on a 2.7-cm diameter phantom tube containing 100 mM aspartate (pH 7.0; 37 °C). NS (No. of scans) = 1024. The results are shown in Fig. 1a–c, LB = 15 Hz. In Fig. 1a, the Gaussian pulse train was placed at 35.2 ppm (control frequency), which partially saturated aspartate C3 at 37.4 ppm. Both aspartate C2 at 53.2 ppm and aspartate C3 at 37.4 ppm were observed. In Fig. 1b, the Gaussian pulse train was placed at the malate C2 frequency (71.2 ppm). In the difference spectrum shown in Fig. 1c, complete cancellation of aspartate C2 was obtained. Fig. 1d–f show the in vivo results of saturating malate C2, LB = 30 Hz. NS = 2688 (summed from two rats for better visualization). In Fig. 1d, the Gaussian pulse train was placed at 35.2 ppm. Glutamate C2 (55.7 ppm), glutamine C2 (55.2 ppm), aspartate C2 (53.2 ppm), GABA C4 + *N*-acetylaspartate C3 (40.4 ppm), aspartate C3 (37.4 ppm), glutamate C4 (34.4 ppm), glutamine C4 (31.9 pm), glutamate C3 (28.0 ppm), glutamine C3 (27.3 ppm) were observed as expected. Fig. 1e shows the in vivo spectrum with the Gaussian pulse train placed at 71.2 ppm. The difference spectrum shown in the bottom trace (Fig. 1f) contains a small but conspicuous signal at the resonance frequency of aspartate C2. In comparison, the nearby much more intense glutamate and glutamine C2 resonances are cancelled in the difference spectrum. Using the MATLAB curve-fitting routine, $[\Delta A]/[A]_0$ was determined to be 0.08 ± 0.01 (means ± SD, $n = 5$, NS = 1152–1536 per rat). Note that the negative signals upfield of aspartate C2 in Fig. 1f were due to saturation of the *N*-acetylaspartate C3, GABA C4, glutamate C4, glutamine C4, glutamate C3 and glutamine C3 resonances by the Gaussian 180° pulse placed at the control frequency. Similar positive signals downfield of aspartate C2 originated from α- and β-glucose C6 resonances were also present (not shown in Fig. 1) because of the Gaussian 180° pulse placed at 71.2 ppm.

As shown previously for chemical exchange between a large pool and a very small pool [13], the longitudinal relaxation time of aspartate C2 measured without RF saturation is essentially the same as that without exchange (T_{1A}). From the inversion-recovery null experiment and taking into account of incomplete longitudinal recovery

$$\left(\exp\left(\frac{T_{1\text{null}}}{T_1}\right)+\exp\left(-\frac{\text{TR}-T_{1\text{null}}}{T_1}\right)=2\right) \quad \text{with TR} = 6.4\,\text{s},$$

T_{1A} was determined to be 2.2 ± 0.1 s (means ± SD, $n = 3$, NS = 1536–2560 per rat). In our previous work [3], V_{AAT} was estimated to be 26 μmol/g wet weight/min by assuming complete RF saturation of oxaloacetate C2 with a nominal γB_{1sat} of 790 Hz and $T_{1A} = T_{1(\text{glutamate C2})}$. Since then, we have repeated the measurement of the oxaloacetate ↔ aspartate CMT effect by reducing γB_{1sat} to 200 Hz and obtained the same amount of magnetization transfer (data not shown), confirming the nearly complete satura-

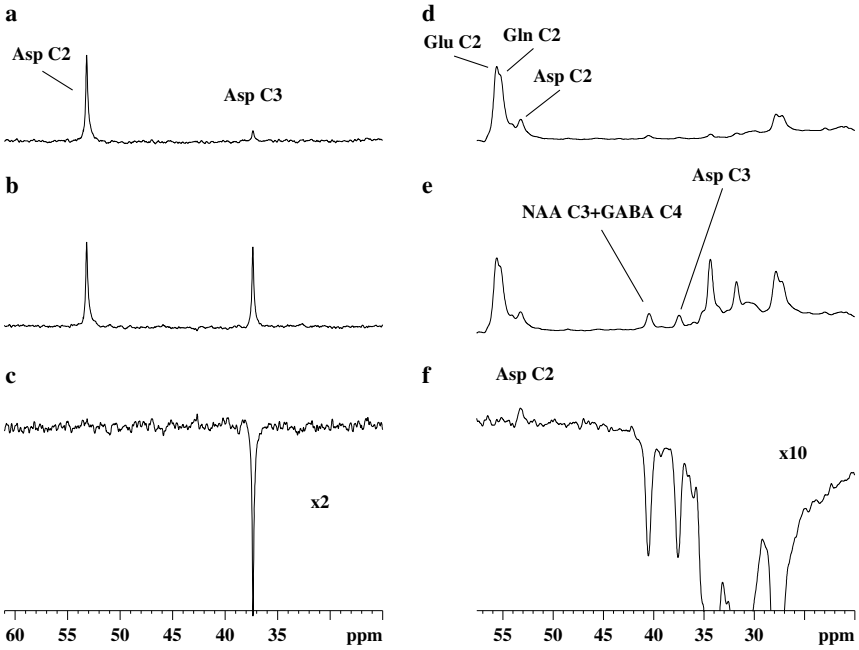

Fig. 1. (a) The Gaussian saturation pulse train was placed at 35.2 ppm (control frequency). NS (No. of scans) = 1024, LB = 15 Hz. A phantom sample containing 100 mM aspartate (pH 7.0; 37 °C) was used. Asp C2, aspartate C2; Asp C3, aspartate C3. (b) The Gaussian pulse train was placed at the malate C2 frequency (71.2 ppm). (c) Difference spectrum. The intensity scale of the difference spectrum was 2× that of the control spectrum. (d) In vivo ^{13}C spectrum with the Gaussian saturation pulse train placed at 35.2 ppm. NS = 2688, LB = 30 Hz. Glu C2, glutamate C2; Gln C2, glutamine C2; Asp C2, aspartate C2. The *N*-acetylaspartate C2 at 54.1 ppm was also observed (unmarked). (e) In vivo ^{13}C spectrum with the Gaussian saturation pulse train placed at 71.2 ppm. GABA C4, γ-aminobutyric acid C4; Asp C3, aspartate C3. (f) The difference spectrum. Asp C2, aspartate C2. The intensity scale of the difference spectrum was 10× that of the control spectrum.

tion of oxaloacetate C2 achieved in our previous work [3]. Using the T_{1A} value determined in the current study, k_{AO} and V_{AAT} were recalculated to be $0.17 \pm 0.02\ s^{-1}$ and 29 ± 4 μmol/g wet weight/min, respectively. From Eq. (8), V_{MDH} was determined to be 9 ± 2 μmol/g wet weight/min (means ± SD, $n = 5$), corresponding to a $t_{1/2}$ time of approximately 1.6 s for malate. Using Eq. (9), $[O]_{ss}/[O]_0$ was calculated to be ~70%.

5. Discussion

Any leakage of perturbed magnetization of oxaloacetate or influx of unperturbed magnetization into oxaloacetate causes an underestimation of V_{MDH} using our relayed magnetization transfer approach. Fortunately, compared to the fast reactions catalyzed by MDH and AAT, all other reactions, involving oxaloacetate are negligibly slow (see below). The association of AAT and MDH or compartmentation of oxaloacetate further reduces leakage of perturbed oxaloacetate magnetization or influx of unperturbed magnetization into oxaloacetate by preventing exchanges between the rest of oxaloacetate and that involved in AAT and MDH reactions [14,15].

In addition to the AAT and MDH reactions, oxaloacetate also participates in reactions catalyzed by pyruvate carboxylase and citrate synthetase, both are located in mitochondria. In mammalian brain, the reversible pyruvate carboxylase reaction is active predominantly in astrocytes [16]. The overall activity of pyruvate carboxylase is negligibly low compared to that of AAT or MDH [16–18], which rules out the possibility of significant interference from the pyruvate carboxylase reaction to the measurement of V_{MDH} using relayed ^{13}C magnetization transfer. The citrate synthetase reaction is essentially irreversible in the forward direction [5]. The upper limit of the leakage of perturbed oxaloacetate magnetization due to the citrate synthetase reaction is, therefore, set by the tricarboxylic acid cycle rate (V_{TCA}). Based on our previously measured V_{TCA} under similar experimental conditions (α-chloralose anesthetized adult rat brain [19]), $V_{TCA}/V_{MDH} \approx 5\%$, which is markedly smaller than the coefficient of variance of the measured V_{MDH}. Furthermore, any effect of leakage of perturbed mitochondrial oxaloacetate magnetization on the predominantly cytosolic aspartate is mitigated by the malate–aspartate shuttle across the mitochondrial inner membrane. As a result, pyruvate carboxylase and citrate synthetase reactions are not expected to have caused any significant errors in the measured V_{MDH}.

Phosphoenolpyruvate carboxykinase in the gluconeogenesis pathway catalyzes the interconversion between oxaloacetate and phosphoenolpyruvate in liver, kidney and adipose tissues. Its activity in brain is essentially undetectable [20]. Oxaloacetate undergoes spontaneous decomposition into pyruvate and carbon dioxide with a first order rate constant of ca. $0.02\ min^{-1}$ at neutral pH [21]. This decomposition reaction is also catalyzed by oxaloacetate decarboxylase, which is active in liver and kidney. In brain, the activity of oxaloacetate decarboxylase was found to be

negligibly low [21]. Leakage of perturbed oxaloacetate magnetization due to oxaloacetate decarboxylase and phosphoenolpyruvate carboxykinase fluxes is therefore negligible. There are also transamination reactions other than the AAT reaction that use oxaloacetate as amino group acceptor. As described earlier [3], the transamination activity in brain is overwhelmingly dominated by that of AAT. These other transamination reactions are not distinguishable from the AAT reaction in magnetization transfer between oxaloacetate and aspartate. Note that the dominant keto form of oxaloacetate [22,23] acts as the substrate for MDH and AAT [15,22]. Chemical exchange between the keto form of oxaloacetate with its minor enol and gem-diol forms does not cause any significant leakage of perturbed magnetization.

Previous in vitro findings using kinetic data for malate dehydrogenase obtained from several species suggest that this enzyme is operating in vivo at well below its K_m values for oxaloacetate and NADH [24,25]. In this study, in vivo V_{MDH} was found to be ~13% of its V_{max} determined from homogenate of rat cerebral cortex [6], providing evidence for the low availability of substrates for this enzyme in vivo.

Finally, the difference in chemical shift between aspartate C2 and malate C2 is 2264 Hz at 11.7 Tesla, significantly greater than the 780 Hz separation between aspartate C3 and malate C3 [26]. The relatively large frequency separation among aspartate, oxaloacetate and malate C2 resonances has made it possible to completely eliminate any RF spill over effect by the use of a spectrally selective Gaussian pulse train for saturating malate C2 (Fig. 1c). Note that malate C2 is coupled to malate H2 with $^1J_{CH} = 146$ Hz (measured from a separate phantom sample containing 100 mM malate, pH 7). The bandwidth of the Gaussian pulse has to be significantly greater than $^1J_{CH}$, preventing the use of very selective RF pulses commonly employed in ^{31}P magnetization transfer MRS studies.

In conclusion, it is demonstrated that the rapid malate dehydrogenase reaction is detectable in vivo using relayed ^{13}C magnetization transfer at 11.7 Tesla. Although measuring MDH reaction at lower magnetic field strength is more difficult, the relay strategy proposed here may be extended to detecting other enzyme-catalyzed reactions and, therefore, providing valuable insight into the catalytic action of enzymes both in vivo and in vitro [27].

Acknowledgment

This work was supported by the intramural research program of the NIH, NIMH.

References

[1] T.R. Brown, Saturation transfer in living systems, Philos. Trans. R. Soc. Lond. B Biol. Sci. 289 (1980) 441–444.
[2] J.R. Alger, R.G. Shulman, NMR studies of enzymatic rates in vitro and in vivo by magnetization transfer, Q. Rev. Biophys. 17 (1984) 83–124.
[3] J. Shen, In vivo carbon-13 magnetization transfer effect. Detection of aspartate aminotransferase reaction, Magn. Reson. Med. 54 (2005) 1321–1326, Erratum in: Magn. Reson. Med. 55 (2006) 713.
[4] S. Xu, J. Yang, J. Shen, In vivo ^{13}C saturation transfer effect of lactate dehydrogenase reaction, Magn. Reson. Med., in press.
[5] B.K. Siesjo, Brain Energy Metabolism, John Wiley & Sons, Chichester, 1978.
[6] L. Ratnakumari, G.Y.C.A. Subbalakshmi, Ch. R.K. Murphy, Acute effects of ammonia on the enzymes of citric acid cycle in rat brain, Neurochem. Intl. 8 (1986) 115–120.
[7] L. Ratnakumari, Ch. R. Murthy, Activities of pyruvate dehydrogenase, enzymes of citric acid cycle, and aminotransferases in the subcellular fractions of cerebral cortex in normal and hyperammonemic rats, Neurochem. Res. 14 (1989) 221–228.
[8] F.A. Middleton, K. Mirnics, J.N. Pierri, D.A. Lewis, P. Levitt, Gene expression profiling reveals alterations of specific metabolic pathways in schizophrenia, J. Neurosci. 22 (2002) 2718–27129.
[9] A.L. Miller, R.A. Hawkins, R.L. Veech, The mitochondrial redox state of rat brain, J. Neurochem. 20 (1973) 1393–1400.
[10] S. Li, J. Shen, Integrated RF probe for in vivo multinuclear spectroscopy and functional imaging of rat brain using an 11.7 Tesla 89 mm bore vertical microimager, MAGMA 18 (2005) 119–127.
[11] Z. Chen, S.S. Li, J. Yang, D. Letizia, J. Shen, Measurement and automatic correction of high-order B_0 inhomogeneity in the rat brain at 11.7 Tesla, Magn. Reson. Imaging 22 (2004) 835–842.
[12] J. Shen, Use of amplitude and frequency transformations to generate adiabatic pulses of wide bandwidth and low RF power deposition, J. Magn. Reson. B 112 (1996) 131–140.
[13] J. Shen, S. Xu, Theoretical analysis of carbon-13 magnetization transfer for in vivo exchange between alpha-ketoglutarate and glutamate, NMR Biomed. 19 (2006) 248–254.
[14] N.C. Price, L. Stevens, Fundamentals of Enzymology, third ed., Oxford University Press, Oxford, 2001.
[15] C.F. Bryce, D.C. Williams, R.A. John, P. Fasella, The anomalous kinetics of coupled aspartate aminotransferase and malate dehydrogenase. Evidence for compartmentation of oxaloacetate, Biochem. J. 153 (1976) 571–577.
[16] R.P. Shank, G.S. Bennett, S.O. Freytag, G.L. Campbell, Pyruvate carboxylase: an astrocyte-specific enzyme implicated in the replenishment of amino acid neurotransmitter pools, Brain Res. 329 (1985) 364–367.
[17] A.C. Yu, J. Drejer, L. Hertz, A. Schousboe, Pyruvate carboxylase activity in primary cultures of astrocytes and neurons, J. Neurochem. 41 (1983) 1484–1487.
[18] J. Butterworth, Changes in nine enzyme markers for neurons, glia, and endothelial cells in agonal state and Huntington's disease caudate nucleus, J. Neurochem. 47 (1986) 583–587.
[19] J. Yang, J. Shen, Increased oxygen consumption in the somatosensory cortex of α-chloralose anesthetized rats during forepaw stimulation determined using MRS at 11.7 Tesla, Neuroimage 32 (2006) 1317–1325.
[20] T.J. Wiese, D.O. Lambeth, P.D. Ray, The intracellular distribution and activities of phosphoenolpyruvate carboxykinase isozymes in various tissues of several mammals and birds, Comp. Biochem. Physiol. B 100 (1991) 297–302.
[21] B. Dean, W. Bartley, Oxaloacetate decarboxylases of rat liver, Biochem. J. 135 (1973) 667–672.
[22] C.I. Pogson, R.G. Wolfe, Oxaloacetic acid. Tautomeric and hydrated forms in solution, Biochem. Biophys. Res. Commun. 46 (1972) 1048–1054.
[23] R.G. Annett, G.W. Kosicki, Oxalacetate keto-enol tautomerase. Purification and characterization, J. Biol. Chem. 244 (1969) 2059–2067.
[24] K.E. Crow, T.J. Braggins, R.D. Batt, M.J. Hardman, Rat liver cytosolic malate dehydrogenase: purification, kinetic properties, role in control of free cytosolic NADH concentration. Analysis of control

of ethanol metabolism using computer simulation, J. Biol. Chem. 257 (1982) 14217–14225.
[25] M. Busquets, J. Baro, A. Cortes, J. Bozal, Separation and properties of the two forms of chicken liver (Gallus domesticus) cytoplasmic malate dehydrogenase, Int. J. Biochem. 10 (1979) 823–835.
[26] T.W.M. Fan, Metabolite profiling by one- and two-dimensional NMR analysis of complex mixtures, Prog. NMR Spectr. 28 (1996) 161–219.
[27] C.R. Malloy, A.D. Sherry, R.L. Nunnally, ^{13}C NMR measurement of flux through alanine aminotransferase by inversion- and aturation-transfer methods, J. Magn. Reson. 64 (1985) 243–254.